Aggregate Morphologies of Amphiphilic ABC Triblock Copolymer in Dilute Solution Using Self-Consistent Field Theory

Rong Wang,*,†,‡ Ping Tang,*,‡ Feng Qiu,‡ and Yuliang Yang‡

Department of Polymer Science and Engineering, College of Chemistry and Chemical Engineering, Nanjing University, Nanjing 210093, China, and Key Laboratory of Molecular Engineering of Polymers, Ministry of Education, and Department of Macromolecular Science, Fudan University, Shanghai 200433, China

Received: June 16, 2005; In Final Form: July 26, 2005

The complex microstructures of amphiphilic ABC linear triblock copolymers in which one of the end blocks is relatively short and hydrophilic, and the other two blocks B and C are hydrophobic in a dilute solution, have been investigated by the real-space implementation of self-consistent field theory (SCFT) in two dimensions (2D). In contrast to diblock copolymers in solution, the aggregation of triblock copolymers are more complicated due to the presence of the second hydrophobic blocks and, hence, big ranges of parameter space controlling the morphology. By tailoring the hydrophobic degree and its difference between the blocks B and C, the various shapes of vesicles, circlelike and linelike micelles possibly corresponding to spherelike, and rodlike micelles in 3D, and especially, peanutlike micelles not found in diblock copolymers are observed. The transition from vesicles to circlelike micelles occurs with increasing the hydrophobicity of the blocks B and C, while the transition from circlelike micelles to linelike micelles or from the mixture of micelles and vesicles to the long linelike micelles takes place when the repulsive interaction of the end hydrophobic block C is stronger than that of the middle hydrophobic block B. Furthermore, it is favorable for dispersion of the block copolymer in the solvent into aggregates when the repulsion of the solvent to the end hydrophobic block is larger than that of the solvent to the middle hydrophobic block. Especially when the bulk block copolymers are in a weak segregation regime, the competition between the microphase separation and macrophase separation exists and the large compound micelle-like aggregates are found due to the macrophase separation with increasing the hydrophobic degree of blocks B and C, which is absent in diblock copolymer solution. The simulation results successfully reproduce the existing experimental ones.

Introduction

The self-assembly of amphiphilic block copolymers in solution into various complex microstructures, such as rod- and spherelike micelles and vesicles, has attracted much attention both experimentally and theoretically in recent years, especially of highly asymmetric diblock or triblock copolymer with minor end blocks into crew-cut aggregates.[1−9] The vesicles formation is of fundamental and practical interests, as they have many potential applications in areas such as microreactors, microcapsules, and drug delivery systems.[10] The solution self-assembly of AB diblock and ABA triblock copolymers is relatively well understood in the past few years.[11−13] Recently, the vesicle and micelle aggregates in solution of complex graft copolymer,[14] star $(AB)_n$,[15] ABC triblock copolymer,[1,16−24] and even ABCA tetrablock copolymer[25] are studied experimentally because of the developments in the field of polymer synthesis. Regarding the applications of the vesicle, control over the size, the shape, and the stability of polymer vesicles is of fundamental importance. Following the ideas of Eisenberg and co-workers,[26−29] the specific morphology is attributed to three contributions of the free energy, including chain stretching in the core, the interfacial energy, and repulsion among corona chains. Therefore, the morphology depends on many factors, such as relative block length, the pH value relating to the solubility of the blocks, the degree of hydrophilic or hydrophobic property of blocks, and so on.

In general, although a number of experimental studies have been carried out to investigate the vesicles in solution, the theoretical study on the complex microstructures of block copolymers in selective solvents is relatively scarce. Guo et al.[7] and van Vlimmeren et al.[8] used dynamic density functional theory to capture the micelle formation of $(EO)_{13}(PO)_{30}(EO)_{13}$ in concentrated solution. Monzen et al.[30] used self-consistent field theory (SCFT) to study the structures and the phase behavior of micelles formed in symmetric and asymmetric ABA and BAB triblock copolymer solutions. They took into account only the spherical micelles, the planar bilayer membranes, and the uniform solutions as the candidates of the possible self-assembled domain structures. But other morphologies, such as spherical vesicles (closed bilayer membranes) and those without higher symmetries, were not included. Recently, the real-space self-consistent field algorithm was applied to study the formation of the mesophases of diblock copolymer in dilute solution in two-dimensional space.[31] By tailoring the interaction parameters and the initial fluctuation, circlelike micelles, linelike micelles, and vesicles were obtained.

However, as the number of distinct blocks is increased from two to three, say, ABC triblock copolymers, both the complexity and variety of self-assembled structures are significantly

* Corresponding authors. E-mail: pingtang@fudan.edu.cn (P.T.); rong_wang73@hotmail.com (R.W.).
† College of Chemistry and Chemical Engineering, Nanjing University.
‡ Key Laboratory of Molecular Engineering of Polymers, Ministry of Education, and Department of Macromolecular Science, Fudan University.

10.1021/jp053248p CCC: $30.25 © 2005 American Chemical Society
Published on Web 08/19/2005

increased. In bulk, the morphologies of ABC triblock copolymer have been studied theoretically[32−35] and experimentally,[36] and the research results show that the microphases not only depend on the composition and the interaction energies between distinct blocks, but also on particular molecular architectures.[32,37] Obviously, the parameter space controlling the morphology of triblock copolymers in solution is remarkably increased, and the presence of an additional hydrophobic block based on the amphiphilic AC or AB diblock copolymer might offer some advantages in the microstructure manipulation.[1] Therefore, distinctively new features absent in diblock copolymers solution arise in triblock copolymers. Because of the structural specificity, the multiple morphologies formed from amphiphilic ABC triblock copolymers in solution are studied experimentally.[1,2,4,25]

In this paper, we use a combinatorial screening method based on the real space implementation of the SCFT, originally proposed by Drolet and Fredrickson for block copolymer melts,[38,39] to search the equilibrium microphases of ABC linear triblock copolymers in dilute solution in 2D. We note that real space solving SCF equations in 3D are still a computationally changing task, and most of the previous work was carried out in 2D. Our computing idea is somewhat different from Liang's;[31,40] we do not press any assumptions on the system, such as the Gaussian distribution initial fluctuation, but only change the segregation degree of blocks and the solubility properties of the blocks to tune the different complex microstructures of linear ABC triblock copolymers in dilute solution. Our method is useful for understanding the formation of aggregates, including vesicles and micelles, as well as the stability of the complex microstructures.

Theoretical Method

In this section, we outline the self-consistent field theory (SCFT) for a mixture of n_p linear ABC triblock copolymers with n_S solvent molecules. Each copolymer chain consists of N segments with compositions (average volume fractions) f_A and f_B ($f_C = 1 - f_A - f_B$), respectively. We assume the mixture is incompressible, with each polymer segment occupying a fixed volume ρ_0^{-1}, and each solvent molecule taking the same volume $v_S = \rho_0^{-1}$. Thus, the total volume of the system is $V = n_pN/\rho_0 + n_Sv_S$, the volume fraction of ABC triblock copolymer is $f_p = n_pN/V\rho_0$, and that of the solvent is $f_S = 1 - f_p$. Furthermore, we assume that the A, B, and C segments have the same statistical length a.

In the SCFT, one considers the statistics of a single copolymer chain in a set of effective chemical potential fields w_i, where i represents block species A, B, C, or solvent S. These chemical potential fields, which represent the actual interactions between different components, are conjugated to the segment density fields, ϕ_i, of different species i. Hence, the free energy (in unit of k_BT) of the system is given by

$$F = -f_p \ln(Q_p/f_pV) - Nf_S \ln(Q_S/f_SV) - 1/V \int d\mathbf{r}[w_A\phi_A + w_B\phi_B + w_C\phi_C + w_S\phi_S + \xi(1 - \phi_A - \phi_B - \phi_C - \phi_S)] + 1/V \int d\mathbf{r}[\chi_{AB}N\phi_A\phi_B + \chi_{AC}N\phi_A\phi_C + \chi_{BC}N\phi_B\phi_C + \chi_{AS}N\phi_A\phi_S + \chi_{BS}N\phi_B\phi_S + \chi_{CS}N\phi_C\phi_S] \quad (1)$$

where χ_{ij} is the Flory−Huggins interaction parameter between species i and j, ξ is the Lagrange multiplier (as a pressure), $Q_p = \int d\mathbf{r}q(\mathbf{r},1)$ is the partition function of a single chain in the effective chemical potential fields w_A, w_B, and w_C, and $Q_S = \int d\mathbf{r} \exp(-w_S(\mathbf{r})/N)$ is the partition function of the solvent in the effective chemical potential field w_S. The fundamental quantity to be calculated in mean field studies is the polymer segment probability distribution function, $q(\mathbf{r},s)$, representing the probability of finding segment s at position $\mathbf{r}$. It satisfies a modified diffusion equation using a flexible Gaussian chain model

$$\frac{\partial}{\partial s}q(\mathbf{r},s) = \frac{Na^2}{6}\nabla^2 q(\mathbf{r},s) - wq(\mathbf{r},s) \quad (2)$$

where w is w_A when $0 < s < f_A$, w_B when $f_A < s < f_A + f_B$, and w_C when $f_A + f_B < s < 1$. The initial condition of eq 2 satisfies $q(\mathbf{r},0) = 1$. Because the two ends of the block copolymer are different, a second distribution function $q^+(\mathbf{r},s)$ is needed that satisfies eq 2 but with the right-hand side multiplied by -1 and the initial condition $q^+(\mathbf{r},1) = 1$. The density of each component is obtained by

$$\phi_A(\mathbf{r}) = \frac{f_pV}{Q}\int_0^{f_A} ds q(\mathbf{r},s)q^+(\mathbf{r},s) \quad (3)$$

$$\phi_B(\mathbf{r}) = \frac{f_pV}{Q}\int_{f_A}^{f_A+f_B} ds q(\mathbf{r},s)q^+(\mathbf{r},s) \quad (4)$$

$$\phi_C(\mathbf{r}) = \frac{f_pV}{Q}\int_{f_A+f_B}^{1} ds q(\mathbf{r},s)q^+(\mathbf{r},s) \quad (5)$$

$$\phi_S(\mathbf{r}) = \frac{f_SV}{Q_S}\exp(-w_S(\mathbf{r})/N) \quad (6)$$

Minimization of the free energy with respect to density and pressure, $\delta F/\delta\phi = \delta F/\delta\xi = 0$, leads to another five equations.

$$w_A(\mathbf{r}) = \chi_{AB}N\phi_B(\mathbf{r}) + \chi_{AC}N\phi_C(\mathbf{r}) + \chi_{AS}N\phi_S(\mathbf{r}) + \xi(\mathbf{r}) \quad (7)$$

$$w_B(\mathbf{r}) = \chi_{AB}N\phi_A(\mathbf{r}) + \chi_{BC}N\phi_C(\mathbf{r}) + \chi_{BS}N\phi_B(\mathbf{r}) + \xi(\mathbf{r}) \quad (8)$$

$$w_C(\mathbf{r}) = \chi_{AC}N\phi_A(\mathbf{r}) + \chi_{BC}N\phi_B(\mathbf{r}) + \chi_{CS}N\phi_S(\mathbf{r}) + \xi(\mathbf{r}) \quad (9)$$

$$w_S(\mathbf{r}) = \chi_{AS}N\phi_A(\mathbf{r}) + \chi_{BS}N\phi_B(\mathbf{r}) + \chi_{CS}N\phi_C(\mathbf{r}) + \xi(\mathbf{r}) \quad (10)$$

$$\phi_A(\mathbf{r}) + \phi_B(\mathbf{r}) + \phi_C(\mathbf{r}) + \phi_S(\mathbf{r}) = 1 \quad (11)$$

Here, we solve eqs 3−11 directly in real space by using a combinatorial screening algorithm proposed by Drolet and Fredrickson.[38,39] The algorithm consists of randomly generating the initial values of the fields $w_i(\mathbf{r})$. By using a Crank−Nicholson scheme and an alternating−direct implicit (ADI) method,[41] the diffusion equations are then integrated to obtain q and q^+, for $0 < s < 1$. Next, the right-hand sides of eqs 3−6 are evaluated to obtain new values for the volume fractions of blocks A, B, C, and solvent S.

The numerical simulations are carried out on the two-dimensional space with a 200×200 square lattice. The grid size is $\Delta x = 0.5$. The simulation is carried out until the phase patterns are stable and the free energy difference between two iterations is smaller than 10^{-5}, i.e., $\Delta F < 10^{-5}$. It should be noted that the resulting aggregates largely depend on the initial fluctuation amplitude. Therefore, our simulation is performed using the same initial fluctuation amplitude value on the order of 10^{-4}, with random uniform distribution to ensure that these obtained different morphologies are not influenced by the initial condition. Furthermore, all the simulation is repeated at least 10 times using different random states and different random numbers to guarantee the structure is not occasionally observed. The concentration of block copolymers is set as $f_p = 0.1$. The end block A is hydrophilic and short enough to ensure the crew-cut aggregates. The degree of the polymerization of block

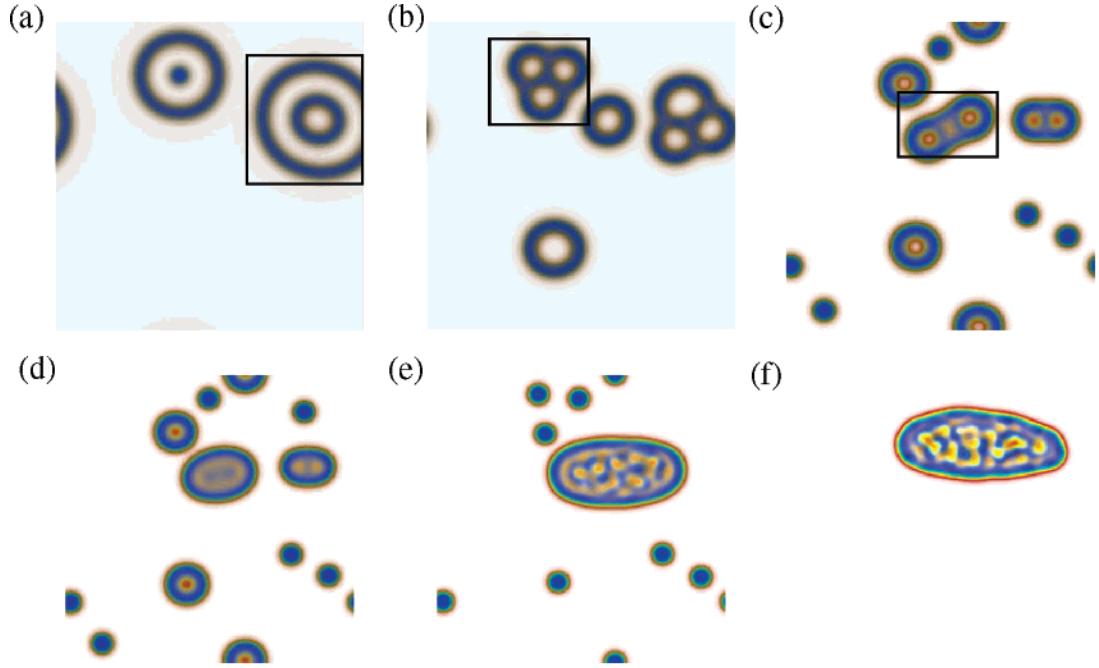

Figure 1. Morphology of amphiphilic ABC triblock copolymer in dilute solution with $\chi = 15$ and $\chi_{AS}N = 0.5$; A (red), B (green), and C (blue). (a) $\chi_{BS}N = \chi_{CS}N = 21.5$, (b) $\chi_{BS}N = \chi_{CS}N = 22$, (c) $\chi_{BS}N = \chi_{CS}N = 25$, (d) $\chi_{BS}N = \chi_{CS}N = 26$, (e) $\chi_{BS}N = \chi_{CS}N = 30$, (f) $\chi_{BS}N = \chi_{CS}N = 40$.

copolymers is $N = 20$, and the composition of block copolymers is taken to be $f_A = 0.1$, $f_B = 0.15$, and $f_C = 0.75$, with the end block C being the major component in all simulations.

Results and Discussion

Because of the complex parameter space as discussed above, in this paper, for the sake of simplicity, the end block A is assumed as hydrophilic and $\chi_{AS}N$ is fixed to be 0.5 and the other two blocks B and C are hydrophobic. Thus, we focus on considering the effect of the hydrophobicity of two blocks B and C of linear ABC block copolymer on the aggregate morphology. We further assume the interaction parameters of the three different blocks are equal, i.e., $\chi_{AB}N = \chi_{AC}N = \chi_{BC}N = \chi$. The morphology is presented with different colors, where red, green, and blue are assigned to A, B, and C blocks, respectively, and the rest are solvents. Similar to the self-assembly of block copolymers in bulk, the segregation degree of different blocks has significant influence on the morphology of block copolymers in solution as well. Consequently, we herein discuss the following two classes in terms of different segregation degree of block copolymers, i.e., weak segregation of linear ABC triblock copolymers in case A and strong segregation of linear ABC triblock copolymers in case B.

A. Weak Segregation of Linear ABC Triblock Copolymers. At the condition $\chi = 15$, the copolymer is in the weak-segregation regime. In this case, the melt of ABC triblock copolymer with $f_A = 0.1$, $f_B = 0.15$, and $f_C = 0.75$ is in a disordered state. But when the solvents are added into the system, the phase behavior changes remarkably.

1. Equal Hydrophobicities of Blocks B and C. When $\chi_{BS}N = \chi_{CS}N$, i.e., the equal hydrophobicities of the blocks B and C, the morphologies of ABC triblock copolymers in dilute solution with increasing of the repulsive interactions between the solvent and blocks B and C are shown in Figure 1. When $\chi_{BS}N$ (or $\chi_{CS}N$) is very small, such as smaller than 21.5, the system is in a disordered state (not shown here). While the vesicles occur when the interaction parameter $\chi_{BS}N(= \chi_{CS}N)$ increases to 21.5, the interface between the solvents and the copolymers is not clear. There is some degree of mixing among the blocks, and thus, microphase separation of block copolymers cannot be observed. With the increase of the degree of the hydrophobic property, the interface between the different blocks is clearly distinguished as shown in Figure 1c. The hydrophilic block A (red) segregates to the inside and outside surface of the vesicles, which is the common phenomena observed in the diblock copolymer system with the minor component of hydrophilic blocks. The vesicles form a three-phase five-layer ABCBA lamellar structure in contrast to the two-phase three-layer ABA lamellar one for diblock copolymers. Figure 2 schematically illustrates the configuration of the vesicle. It is interesting to note that these different vesicles have been observed in PS−PEO diblock copolymer solution,[5] and the only difference is the number of the layers comprising the vesicles. Furthermore, Eisenberg reported the similar spherical vesicles prepared from $PS_{180}-PMMA_{67}-PtBuA_{37}$ linear triblock copolymer solution.[1] The observed specific vesicles (in the pane) in Figure 1a−c are called pregnant, star fish-like, and budding vesicles, respectively, from Eisenberg's notation.[5] But with further increasing $\chi_{BS}N(= \chi_{CS}N)$, which means that the solubility for blocks B and C decreases, the solvent cannot mix with the blocks B and C, and the interfacial tension goes up, then the block copolymer tends to macroseparate from the solvent and thus forms large-size micellar aggregates. Once the interactions between the solvent and the hydrophobic blocks B and C

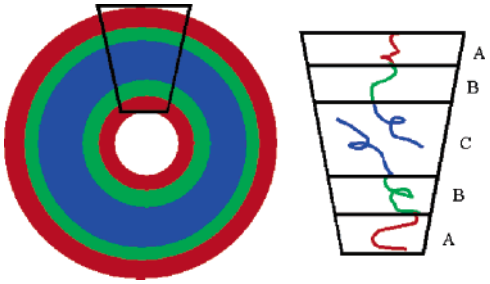

Figure 2. Schematic of a vesicle formed by amphiphilic ABC triblock copolymer in dilute solution. Cutout of a small section of the configuration of the vesicle is shown in the right.

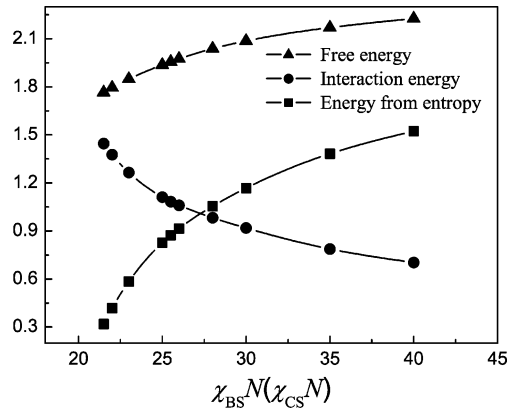

Figure 3. Free energy F (triangles), interaction energy (spheres), and energy from entropy (squares) in unit of k_BT as a function of $\chi_{BS}N(=\chi_{CS}N)$ with $\chi = 15$ and $\chi_{AS}N = 0.5$.

become very strongly repulsive, the repulsive forces between the A, B, and C blocks cannot balance the repulsion from the solvent, therefore, the hydrophobic block C prefers to self-assemble into the inner part of the phase to completely avoid the contact with the solvents, then the system will macroseparate. It should be pointed out that the phenomena due to the competition between macrophase and microphase separation existing in a linear ABC triblock copolymer system, however, are absent for diblocks.

To illustrate the thermodynamic stability of the aggregate morphologies, the calculated free energy based on eq 1 is presented in Figure 3. In eq 1, the first three terms of the right-hand side give the entropy, and the last term gives the enthalpic or the interaction contribution to the free energy. Figure 3 plots the calculated free energy F (triangles), the interaction energy (spheres), and the energy from entropy (squares) in units of k_BT as a function of $\chi_{BS}N(=\chi_{CS}N)$. From Figure 3, we can see the free energy and the energy contributed from entropy increase with $\chi_{BS}N(=\chi_{CS}N)$ increasing, while the interaction energy decreases. At the condition of weak repulsive interactions between the solvent and the hydrophobic blocks B and C, the interaction energy dominates the aggregation process, which corresponds to the microphase separation, resulting in the formation of the vesicles, shown in Figure 1a−c. Here, we can conclude that the vesicles are stable microstructures as their free energies are the lowest, while the entropies are the largest. With $\chi_{BS}N(=\chi_{CS}N)$ increasing, there is a stage that the interaction energy and the energy from entropy are comparable, which corresponds to the coexisting of the microseparated state with the macr-separated state, shown in Figure 1d and e. With further increasing $\chi_{BS}N(=\chi_{CS}N)$, i.e., the high degree of the hydrophobic property, the system will only macroseparate and form large compound micelles as shown in Figure 1f. Therefore, we tailor the values of $\chi_{BS}N(=\chi_{CS}N)$ to design the morphologies of aggregates, including various shapes of vesicles and large compound micelles due to macroseparated block copolymers from the solvents.

2. Nonequal Hydrophobicities of Blocks B and C. In this section, we investigate the effect of the difference of the hydrophobicity between blocks B and C on the self-assembled morphology. Because of the specific sequence characteristics of the middle blocks B for linear ABC triblock copolymers, the hydrophobic degree of the middle blocks has a large influence on the aggregate morphologies. To illustrate this, we first fix the interaction parameter between the middle block B and the solvent $\chi_{BS}N$ to be 10, i.e., the block B is weakly hydrophobic. The morphologies are shown in Figure 4 for $\chi = 15$, $\chi_{AS}N = 0.5$ with changing $\chi_{CS}N$. In this case, the blocks A and B prefer to form a hydrophilic part. When $\chi_{CS}N$ is smaller than 24, the system is in a disordered state. With $\chi_{CS}N$ increasing to 24, the vesicles are formed, as shown in Figure 4a. The linelike micelles and circlelike micelles are observed as $\chi_{CS}N$ increasing. The open vesicle emerges as the vesicles change to micelles. It should be pointed out that further decreasing $\chi_{BS}N$, such as $\chi_{BS}N = 0.5$, i.e., the middle block B is hydrophilic, similar aggregate morphologies (not shown) are also found. It is interesting that the long rodlike micelles were experimentally found in dilute $PS_{310}-PAA_{52}$ diblock copolymer solution,[27,28] and also the vesicle-to-rod transition was observed.[28,29] In fact, in this case, the short blocks A and B form a relatively hydrophilic part because of the weak segregation degree of the block copolymers. As a consequence, the aggregate morphologies from this kind of ABC triblock copolymers are quite similar to those from amphiphilic AB diblock copolymers.

Second, we check the effects of different hydrophobicity of blocks B and C on the morphologies when the middle block B is strongly hydrophobic. For example, for $\chi_{BS}N = 30$, the morphologies are shown in Figure 5 for $\chi = 15$, $\chi_{AS}N = 0.5$. When $\chi_{CS}N < \chi_{BS}N$, i.e., the middle block B is most hydrophobic, the weaker hydrophobic block C, which is the major component of the copolymer, tends to partially mix with hydrophilic block A. As a response, the microphase separation exists at the interface between the solvent and the block copolymer, resulting in obscure interface between the block copolymer and the solvent. In this case, large compound micelles are observed, and the block copolymers are in a disordered state due to the weak segregation degree of the block copolymer. With increasing of the hydrophobicity of the block C, the boundaries both among the different blocks and between the copolymer and the solvent become distinguished and develop a core−shell−shell structure of the block copolymer, then the coexisting of large compound micelles with the general small micelles occurs, as shown in Figure 5b and c. But when $\chi_{CS}N$ further increases to larger than $\chi_{BS}N$, i.e., $\chi_{CS}N > \chi_{BS}N$, the long linelike micelles are found, as shown in Figure 5d and e. We note that the long rodlike micelles were also experimentally found in dilute $PS_{310}-PAA_{52}$ diblock copolymer solution.[27,28] Therefore, it is favorable for the dispersion of the polymer in the solvents, forming circlelike or linelike micelles when $\chi_{CS}N > \chi_{BS}N \gg \chi_{AS}N$, while macrophase separation occurs and forms large compound micelles when $\chi_{CS}N < \chi_{BS}N$. In Figure 5, with improving of the solvent solubility for the core block C, the aggregate morphologies follow the order of e → d → c → b → a, i.e., from line to circle aggregates. Therefore, the better the solubility of the core block C is, the more likely the system forms the circlelike aggregates, in agreement with the experimental results reported by Eisenberg et al.[42,43]

Figure 6 shows the free energy F (triangles), the interaction energy (spheres), and the energy from entropy (squares) as a function of $\chi_{CS}N$ for the case of weak and strong hydrophobicities of the middle blocks B, respectively. When $\chi_{CS}N$ is relatively small, the interaction energy dominates the self-assembled process, while the energy from the entropy dominates at larger $\chi_{CS}N$. When $\chi_{CS}N > \chi_{BS}N \gg \chi_{AS}N$, the favorable dispersion of block copolymers into the solvent occurs, and thus, there is some degree of mixing between blocks B (A) and the solvent. But when $\chi_{CS}N \cong \chi_{BS}N \gg \chi_{AS}N$ for $\chi_{BS}N = 30$, the interaction energy and the energy from entropy are comparable, which corresponds to the coexisting of the microphase separation with marophase separation.

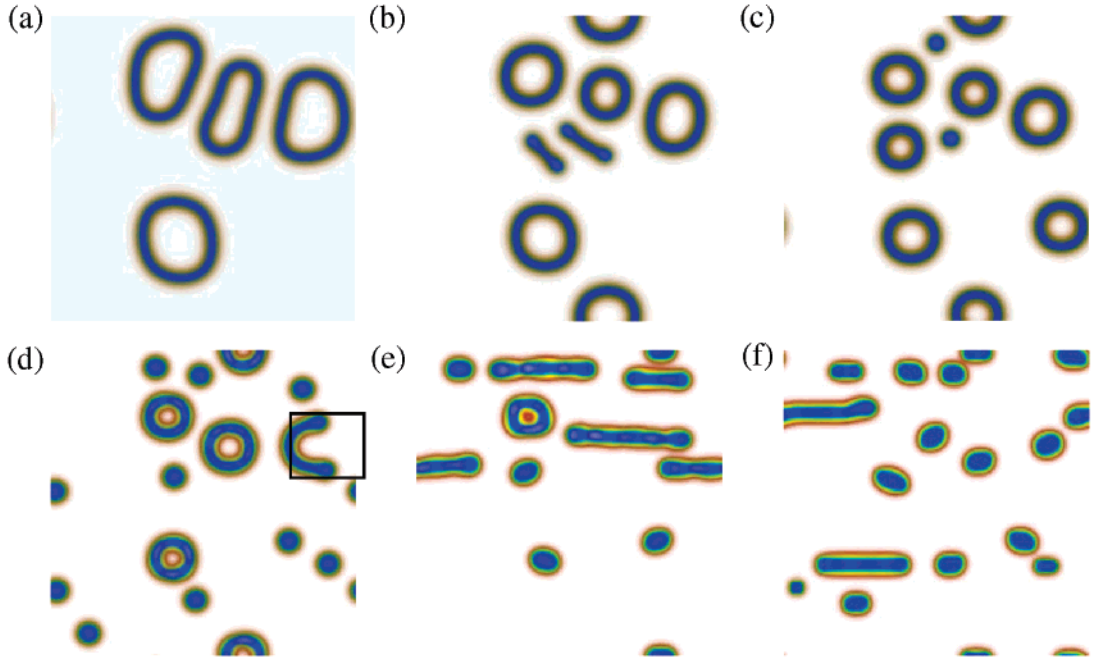

Figure 4. Morphology of amphiphilic ABC triblock copolymer in dilute solution with $\chi = 15$, $\chi_{AS}N = 0.5$, and $\chi_{BS}N = 10$; A (red), B (green), and C (blue). (a) $\chi_{CS}N = 24$, (b) $\chi_{CS}N = 24.5$, (c) $\chi_{CS}N = 25$, (d) $\chi_{CS}N = 30$, (e) $\chi_{CS}N = 38$, (f) $\chi_{CS}N = 45$.

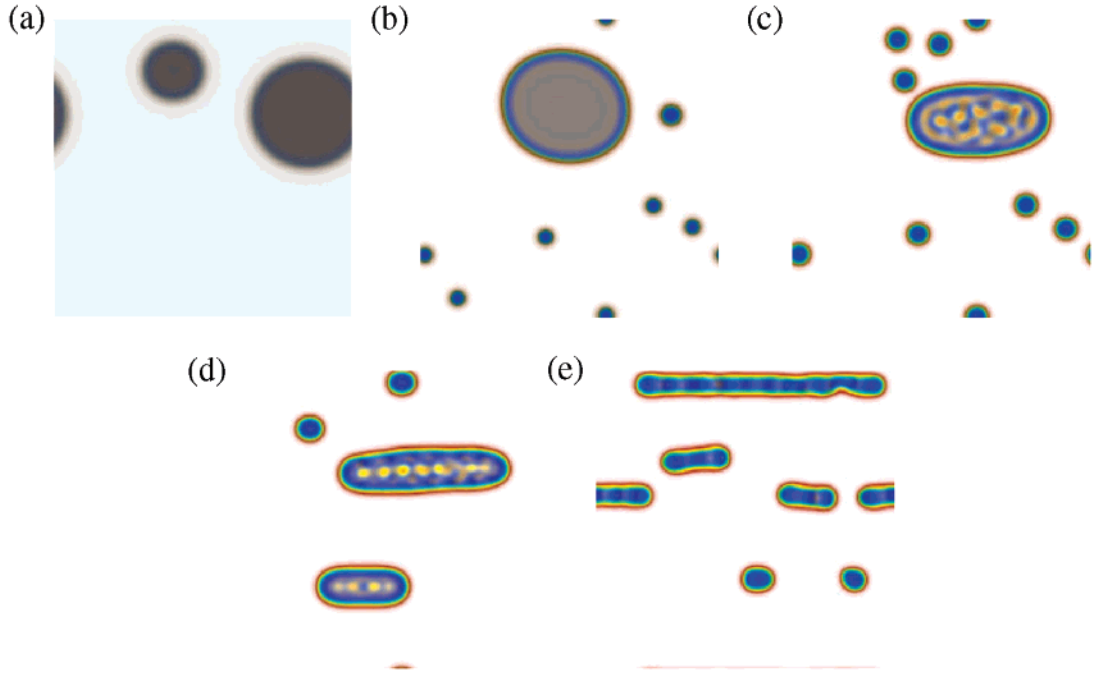

Figure 5. Morphology of amphiphilic ABC triblock copolymer in dilute solution with $\chi = 15$, $\chi_{AS}N = 0.5$, and $\chi_{BS}N = 30$; A (red), B (green), and C (blue). (a) $\chi_{CS}N = 20$, (b) $\chi_{CS}N = 25$, (c) $\chi_{CS}N = 30$, (d) $\chi_{CS}N = 35$, (e) $\chi_{CS}N = 40$.

From the above discussions, we conclude that, in the weak segregation regime for linear ABC triblock copolymer, the macrophase separation occurs, forming large compound micelles when the middle block is the most hydrophobic part, while the vesicle-to-micelle transition is observed with the increasing of hydrophobicity of the end block C when the middle block B is weakly hydropholibic. The favorable case for the dispersion of the block copolymer in the solvent into the vesicles and micelles is that the hydrophobicity of the block C is larger than that of the block B, i.e., $\chi_{CS}N > \chi_{BS}N \gg \chi_{AS}N$.

B. Strong Segregation of Linear ABC Triblock Copolymers. In contrast to the case A here, we consider the case for the stronger segregation degree of ABC triblock copolymer, for example, $\chi = 35$. In this case, the microstructure of ABC triblock copolymer melt is a core−shell hexagonal lattice (CSH).[32] As many solvents are added into the copolymers, however, the aggregate morphologies become more complex due to the phase separation competition between the block copolymer and the solvents.

Similar to the case A, i.e., the block copolymer is in the weak segregation regime, we first discuss the case when $\chi_{BS}N = \chi_{CS}N$. The aggregate morphologies are shown in Figure 7 as we increase the hydrophobicities of the blocks B and C synchronously. The microstructures change from vesicles to circlelike micelles, then to peanutlike micelles, and finally, to micelles. When the hydrophobicity is not strong enough, the system is

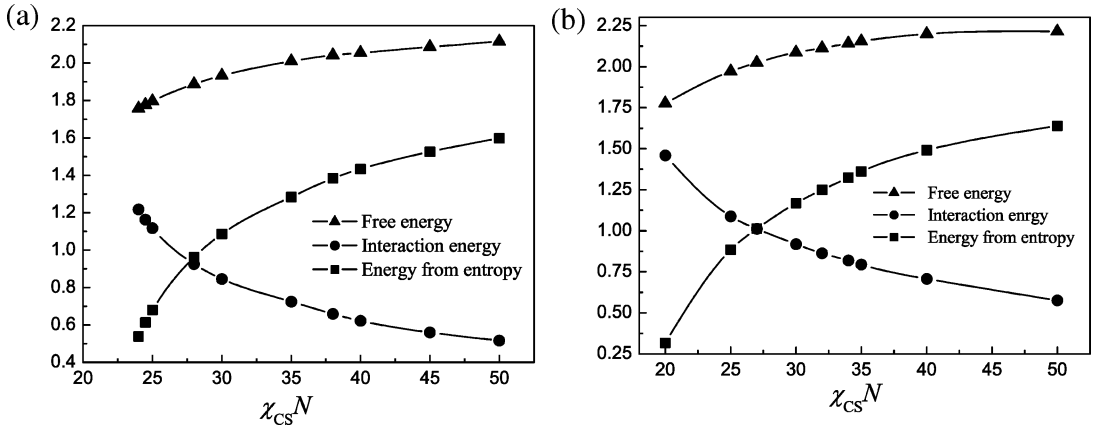

Figure 6. Free energy F (triangles), interaction energy (spheres) and energy from entropy (squares) in unit of k_BT as a function of $\chi_{CS}N$ with $\chi = 15$, $\chi_{AS}N = 0.5$. (a) $\chi_{BS}N = 10$, (b) $\chi_{BS}N = 30$.

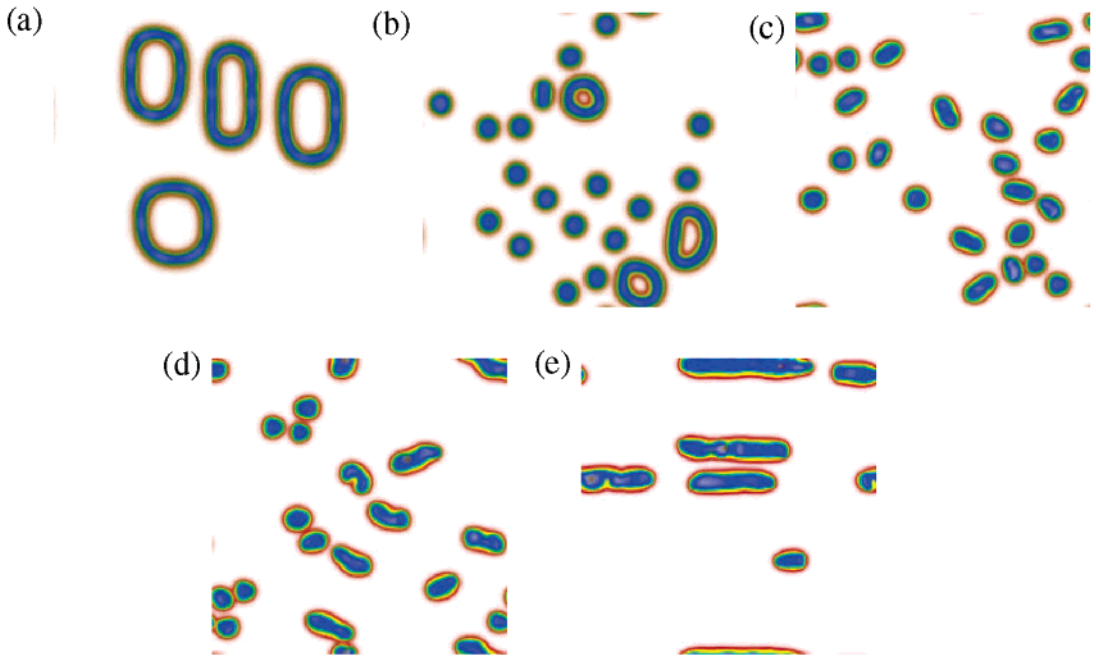

Figure 7. Morphology of amphiphilic ABC triblock copolymer in dilute solution with $\chi = 35$ and $\chi_{AS}N = 0.5$; A (red), B (green), and C (blue). (a) $\chi_{BS}N = \chi_{CS}N = 26$, (b) $\chi_{BS}N = \chi_{CS}N = 28$, (c) $\chi_{BS}N = \chi_{CS}N = 35$, (d) $\chi_{BS}N = \chi_{CS}N = 40$, (e) $\chi_{BS}N = \chi_{CS}N = 50$.

in a disordered state (not shown here). The vesicles occur when $\chi_{BS}N(= \chi_{CS}N)$ increase to 26, see Figure 7a. The micelles emerge with $\chi_{BS}N(= \chi_{CS}N)$ increasing because of the stronger repulsion of the solvent, and then the vesicles coexist with the circlelike micelles. From Figure 7c and d, we can see that the peanutlike micelles as the hydrophobicities of blocks B and C further increase. The linelike micelles (Figure 7e) occur when the repulsive interaction between the blocks B (C) and the solvent is strong. It is important to note that, compared to the case A in Figure 1, the macrophase separation does not exist, while peanutlike and long linelike micelles occur instead in this case because of the relatively strong interactions among the different blocks. However, the weak hydrophobic condition favors the vesicle formation similar to the case A. The vesicle-to-circlelike micelle transition is found with increasing the hydrophobicities of the blocks B and C.

Second, when the hydrophobicities of the blocks B and C are not the same, i.e., $\chi_{BS}N \neq \chi_{CS}N$, the morphology will change with the relative values of $\chi_{BS}N$ and $\chi_{CS}N$. At first, we consider the case that the middle block B is weakly hydrophobic. Figure 8 presents the morphology for $\chi = 35$, $\chi_{AS}N = 0.5$, and $\chi_{BS}N = 10$. The vesicles are first observed with the increase of $\chi_{CS}N$. Then, the vesicles will open to form the linelike micelles and the circlelike micelles with further increase of the hydrophobicity of the block C and, last, to circlelike micelles. Compared to the case A in Figure 4, small circlelike micelles with narrow size distribution is obtained in Figure 8. Following Eisenberg's idea[3] for small vesicles, the interfacial area is strongly size-dependent and, thus, resulting in narrow size distribution.

Subsequently, we fix $\chi_{BS}N$ at 30 to ensure the middle block B is strongly hydrophobic. The aggregate morphologies for $\chi = 35$, $\chi_{AS}N = 0.5$, and $\chi_{BS}N = 30$ are shown in Figure 9 with the hydrophobicity of the block C increasing. The system is in a disordered state when $\chi_{CS}N < 26$. With the solubility of the block C decreasing ($\chi_{CS}N$ increasing), the mixture of vesicles and circlelike micelles are first observed (Figure 9a) when $\chi_{CS}N \leq \chi_{BS}N$. Then, with further increasing the hydrophobicity of the block C larger than that of the block B, the microstructures change to circlelike micelles and then to linelike micelles. We note that when the hydrophobicity of the block B is very strong, the linelike micelles are found, while small circlelike micelles are observed for the case when the middle block is weakly

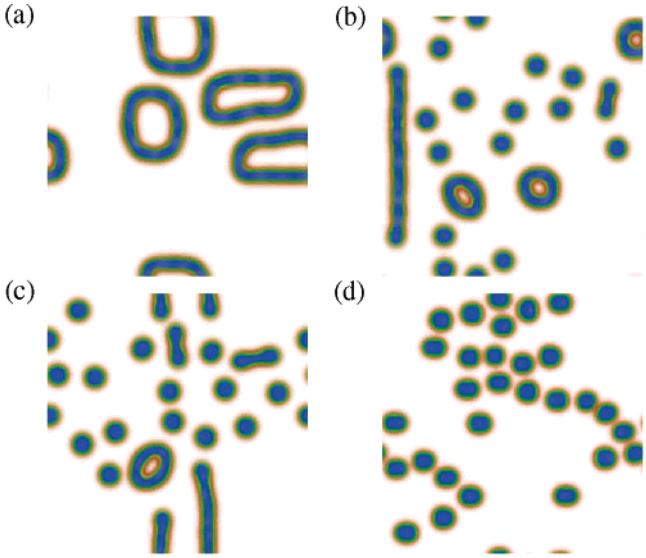

Figure 8. Morphology of amphiphilic ABC triblock copolymer in dilute solution with $\chi = 35$, $\chi_{AS}N = 0.5$, and $\chi_{BS}N = 10$; A (red), B (green), and C (blue). (a) $\chi_{CS}N = 28.3$, (b) $\chi_{CS}N = 29$, (c) $\chi_{CS}N = 30$, (d) $\chi_{CS}N = 35$.

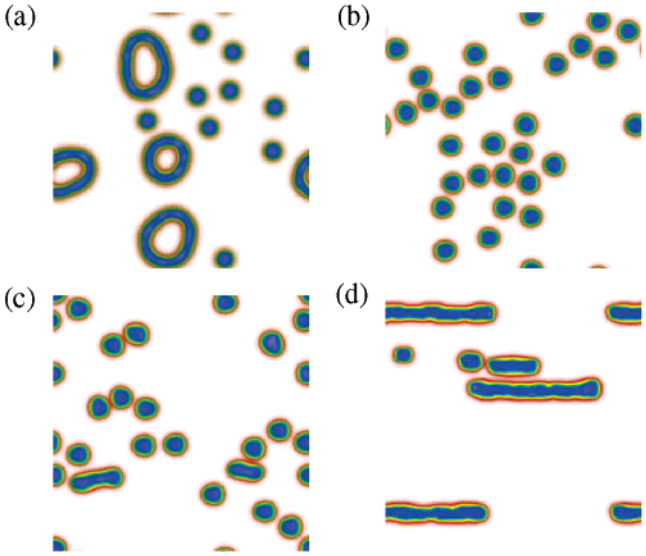

Figure 9. Morphology of amphiphilic ABC triblock copolymer in dilute solution with $\chi = 35$, $\chi_{AS}N = 0.5$, and $\chi_{BS}N = 30$; A (red), B (green), and C (blue). (a) $\chi_{CS}N = 26$, (b) $\chi_{CS}N = 35$, (c) $\chi_{CS}N = 37$, (d) $\chi_{CS}N = 60$.

hydrophobic. It is interesting that the transition both from sphere-to-rod and rod-to-sphere was observed in ternary system $PS_{310}-PAA_{52}$/dioxane/water.[27] In general, the transition from spherelike (circlelike) micelles to rodlike (linelike) micelles is more favorable, as it leads to a decrease in the interfacial area between the solvent and the chains of the inner part of the aggregates, but it will accompany an increase in the stretching of the inner chains (block C) of the micelles. The balance between the two effects results in the free energy of the system. However, the stretching of the inner chains has greater influence on the energy of the system than the decrease in the interfacial area or the increase in the corona repulsion.[44,45] Figures 3 and 6 clearly confirm the point. As the circlelike micelles change to linelike micelles, additional freedom is gained along the long axis with little change in the conformation of the copolymer chains. Therefore, the linelike micelles are stable when the hydrophobicity of the block C is very large.

Summary

By using the 2D real-space SCFT algorithm, an ABC linear triblock copolymer with two hydrophobic blocks B and C of different block lengths and relatively short hydrophilic block A in dilute solution can form circlelike, linelike, especially peanutlike micelles and various shapes of vesicles, depending on the hydrophobic degree and its difference between blocks B and C. Compared to the diblock copolymer solution, the aggregate morphologies have a core−shell−shell structure for the circlelike micelles, and a three-phase five-layer ABCBA lamellar structure for the vesicles, with hydrophilic block A forming the corona. It is based on the fact that, in solution, the C block aggregates first, which is then followed by the aggregation of the B during the micellization of the copolymer as described above. Furthermore, blocks C and B are likely to be phase separated, depending on interaction parameters between the two blocks. Among these aggregate morphologies, vesicles are stable only when the hydrophobilicity of blocks B and C is relatively weak.

In this paper, we consider two classes in terms of phase segregation degree of bulk triblock copolymers and focus on the effect of the hydrophobic degree and its difference between two hydrophobic blocks on the self-assembled morphologies. In a weak segregation state of the block copolymer, there exists the competition between the macrophase separation and microphase separation, which is absent in diblock copolymer solution. When the hydrophobicities of the blocks B and C are equal, the aggregate morphologies will change from vesicles, to the mixture of vesicles and micelles, to micelles, and last, to macrophase separation forming large compound micelles. It should be pointed out that only when the middle block B is strongly hydrophobic is the macrophase separation existing between the polymer and the solvent observed, and thus, large compound micelles are found. It is favorable for dispersion of the block copolymer in the solvent when $\chi_{CS}N > \chi_{BS}N \gg \chi_{AS}N$ and the transition of the mixture of micelles and vesicles to the long linelike micelles takes place with the difference between $\chi_{CS}N$ and $\chi_{BS}N$ increasing.

When the interaction parameters between the three different blocks increase to a strong segregation state, only the microphase separation exists with varying the hydrophobicities of the blocks B and C. When $\chi_{BS}N > \chi_{CS}N$, the peanutlike micelles and necklace structure occur with the difference between $\chi_{CS}N$ and $\chi_{BS}N$ increasing. But the linelike micelles, the circlelike micelles, and the vesicles or their mixtures will form if $\chi_{BS}N < \chi_{CS}N$. The long linelike micelles will form when the middle block B is strongly hydrophobic, while the circlelike micelles occur when the middle block B is weakly hydrophobic, as the hydrophobicity of the block C is very large.

Acknowledgment. We acknowledge financial support from the Special Funds for Major State Basic Research Projects (Grant no. 2005CB623800) and from the Excellent Research Group of NSF of China. The NSF of China (Grant Nos. 20474012, 20374016 and 20104002) is also acknowledged. R. W. acknowledges financial support from Nanjing University Talent Development Foundation (No. 0205004107), Natural Science Foundation of Nanjing University (No. 0205005216) and the Opening Research Foundation of the Key Laboratory of Molecular Engineering of Polymer of Fudan University, Ministry of Education.

References and Notes

(1) Yu, G.; Eisenberg, A. *Macromolecules* **1998**, *31*, 5546.
(2) Luo, L. B.; Eisenberg, A. *J. Am. Chem. Soc.* **2001**, *123*, 1012.

(3) Luo, L. B.; Eisenberg, A. *Langmuir* **2001**, *17*, 6804.
(4) Liu, F. T.; Eisenberg, A. *J. Am. Chem. Soc.* **2003**, *125*, 15059.
(5) Yu, K.; Eisenberg, A. *Macromolecules* **1998**, *31*, 3509.
(6) Burke, S.; Shen, H. W.; Eisenberg, A. *Macromol. Symp.* **2001**, *175*, 273.
(7) Guo, S. L.; Hou, T. J.; Xu, X. J. *J. Phys. Chem. B* **2002**, *106*, 11397.
(8) van Vlimmeren, B. A. C.; Maurits, N. M.; Zvelindovsky, A. V.; Sevink, G. J. A.; Fraaije, J. *Macromolecules* **1999**, *32*, 646.
(9) Bryskhe, K.; Jansson, J.; Topgaard, D.; Schillen, K.; Olsson, U. *J. Phys. Chem. B* **2004**, *108*, 9710.
(10) Allen, C.; Maysinger, D.; Eisenberg, A. *Colloids Surf. B.* **1999**, *16*, 3.
(11) Tuzar, Z.; Kratochvil, P. *Surface and Colloid Science*; Plenum Press: New York, 1993; Vol. 15.
(12) Hamley, I. W. *The Physics of Block Copolymers*; Oxford University Press: New York, 1998.
(13) Riess, G. *Prog. Polym. Sci.* **2003**, *28*, 1107.
(14) Borisov, O. V.; Zhulina, E. B. *Macromolecules* **2005**, *38*, 2506.
(15) Mountrichas, G.; Mpiri, M.; Pispas, S. *Macromolecules* **2005**, *38*, 940.
(16) Dormidontova, E. E.; Khokhlov, A. R. *Macromolecules* **1997**, *30*, 1980.
(17) Zhou, Z. L.; Li, Z. B.; Ren, Y.; Hillmyer, M.; Lodge, T. P. *J. Am. Chem. Soc.* **2003**, *125*, 10182.
(18) Kriz, J.; Masar, B.; Plestil, J.; Tuzar, Z.; Pospisil, H.; Doskocilova, D. *Macromolecules* **1998**, *31*, 41.
(19) Liu, S. Y.; Armes, S. P. *J. Am. Chem. Soc.* **2001**, *123*, 9910.
(20) Gohy, J. F.; Willet, N.; Varshney, S.; Zhang, J. X.; Jerome, R. *Angew. Chem., Int. Ed.* **2001**, *40*, 3214.
(21) Bieringer, R.; Abetz, V.; Muller, A. H. E. *Eur. Phys. J. E* **2001**, *5*, 5.
(22) Butun, V.; Wang, X. S.; Banez, M. V. D.; Robinson, K. L.; Billingham, N. C.; Armes, S. P.; Tuzar, Z. *Macromolecules* **2000**, *33*, 1.
(23) Patrickios, C. S.; Lowe, A. B.; Armes, S. P.; Billingham, N. C. *J. Polym. Sci., Part A, Polym. Chem.* **1998**, *36*, 617.
(24) Sfika, V.; Tsitsilianis, C.; Kiriy, A.; Gorodyska, G.; Stamm, M. *Macromolecules* **2004**, *37*, 9551.
(25) Brannan, A. K.; Bates, F. S. *Macromolecules* **2004**, *37*, 8816.
(26) Luo, L. B.; Eisenberg, A. *Langmuir* **2002**, *18*, 1952.
(27) Burke, S. E.; Eisenberg, A. *Langmuir* **2001**, *17*, 6705.
(28) Chen, L.; Shen, H. W.; Eisenberg, A. *J. Phys. Chem. B* **1999**, *103*, 9488.
(29) Burke, S. E.; Eisenberg, A. *Polymer* **2001**, *42*, 9111.
(30) Monzen, M.; Kawakatsu, T.; Doi, M.; Hasegawa, R. *Comput. Theor. Polym. Sci.* **2000**, *10*, 275.
(31) He, X. H.; Liang, H. J.; Huang, L.; Pan, C. Y. *J. Phys. Chem. B* **2004**, *108*, 1731.
(32) Tang, P.; Qiu, F.; Zhang, H. D.; Yang, Y. L. *Phys. Rev. E* **2004**, *69*, 031803.
(33) Matsen, M. W. *J. Chem. Phys.***1998**, *108*, 785.
(34) Zheng, W.; Wang, Z. G. *Macromolecules* **1995**, *28*, 7215.
(35) Matsen, M. W.; Schick, M. *Curr. Opin. Colloid Interface Sci.* **1996**, *1*, 329.
(36) Lohse, D. J.; Hadjichristidis, N. *Curr. Opin. Colloid Interface Sci.* **1997**, *2*, 171.
(37) Tang, P.; Qiu, F.; Zhang, H. D.; Yang, Y. L. *J. Phys. Chem. B* **2004**, *108*, 8434.
(38) Drolet, F.; Fredrickson, G. H. *Phys. Rev. Lett.* **1999**, *83*, 4317.
(39) Drolet, F.; Fredrickson, G. H. *Macromolecules* **2001**, *34*, 5317.
(40) Zhu, J. T.; Jiang, Y.; Liang, H. J.; Jiang, W. *J. Phys. Chem. B* **2005**, *109*, 8619.
(41) Press, W. H.; Flannery, B. P.; Teukolsky, S. A.; Vettering, W. T. *Numerical Recipes*; Cambridge Univeristy Press: Cambridge, 1989.
(42) Desbaumes, L.; Eisenberg, A. *Langmuir* **1999**, *15*, 36.
(43) Yu, Y.; Eisenberg, A. *J. Am. Chem. Soc.* **1997**, *119*, 8383.
(44) Shen, H. W.; Eisenberg, A. *Macromolecules* **2000**, *33*, 2561.
(45) Zhang, L. F.; Eisenberg, A. *Macromolecules* **1999**, *32*, 2239.